Published in final edited form as:
Matrix Biol. 2011 April ; 30(3): 178–187. doi:10.1016/j.matbio.2010.12.002.

Lysyl oxidase-like 3b is Critical for Cartilage Maturation During Zebrafish Craniofacial Development

Antonius L. van Boxtel[1,2,†], **John M. Gansner**[3], **Henk W.J. Hakvoort**[1], **Heather Snell**[4], **Juliette Legler**[1], and **Jonathan D. Gitlin**[4]

[1]Institute for Environmental Studies, VU University, Amsterdam, The Netherlands [3]Washington University School of Medicine, St. Louis, MO, USA [4]Department of Pediatrics, Vanderbilt University School of Medicine, Nashville, TN, USA

Abstract

Vertebrate craniofacial development requires coordinated morphogenetic interactions between the extracellular matrix (ECM) and the differentiating chondrocytes essential for cartilage formation. Recent studies reveal a critical role for specific lysyl oxidases in ECM integrity required for embryonic development. We now demonstrate that *loxl3b* is abundantly expressed within the head mesenchyme of the zebrafish and is critically important for maturation of neural crest derived cartilage elements. Histological and ultrastructural analysis of cartilage elements in *loxl3b* morphant embryos reveals abnormal maturation of cartilage and altered chondrocyte morphology. Spatiotemporal analysis of craniofacial markers in *loxl3b* morphant embryos shows that cranial neural crest cells migrate normally into the developing pharyngeal arches but that differentiation and condensation markers are aberrantly expressed. We further show that the *loxl3b* morphant phenotype is not due to P53 mediated cell death but likely to be due to reduced chondrogenic progenitor cell proliferation within the pharyngeal arches. Taken together, these data demonstrate a novel role for *loxl3b* in the maturation of craniofacial cartilage and can provide new insight into the specific genetic factors important in the pathogenesis of craniofacial birth defects.

Keywords

zebrafish; lysyl oxidase; cartilage; craniofacial development

1. Introduction

The development of the vertebrate craniofacial skeleton is a complex process that requires migration of neural crest cells (NCCs) into the pharyngeal arches and subsequent epitheliomesenchymal interactions for condensation, fate determination and terminal differentiation (Hall and Miyake 2000;Helms and Schneider 2003;Goldring et al. 2006;Szabo-Rogers et al. 2009). Chondrocyte differentiation within pharyngeal arch condensations is controlled by tightly regulated soluble factors secreted by surrounding

[†]Corresponding Author: Antonius L. van Boxtel, PhD, Laboratory of Developmental Signaling, Cancer Research UK London Research Institute, 44 Lincoln's Inn Fields, London WC2A 3PX, United Kingdom, Thijs.vanBoxtel@cancer.org.uk.
[2]Current address: Cancer Research UK London Research Institute, London, United Kingdom

endoderm and ectoderm and by cell-cell and cell-extracellular matrix (ECM) interactions (Goldring et al. 2006;Woods et al. 2007). As such, chondrogenic progenitor cells are dependent on the proper deposition of the ECM for proliferation and overt differentiation. Genetic and environmental factors that compromise the ECM result in craniofacial pathogenesis but the exact molecular interactions of chondrogenic progenitor cells with the ECM required for chondrogenesis are poorly understood (Woods et al. 2007;Goldring et al. 2006).

The lysyl oxidases are a family of evolutionary conserved cuproenzymes that modify the ECM (Lucero and Kagan 2006). In mammals, five lysyl oxidases have been described: the prototypic lysyl oxidase (LOX) and the sequentially numbered lysyl oxidase-like (LOXL) proteins LOXL1, LOXL2, LOXL3, and LOXL4 (Lucero and Kagan 2006;Maki 2009). Lysyl oxidase family members consist of a conserved C-terminal domain containing a copper binding motif and a lysyl oxidase catalytic domain, as well as a more variable N-terminal domain which in the case of LOXL2-4 contains multiple scavenger receptor, cysteine-rich (SRCR) domains (Maki 2009). The catalytic domain deaminates ε-lysine residues into highly reactive allysine residues, permitting intra- and inter-molecular cross-link formation in proteins (Lucero and Kagan 2006;Maki 2009). Based on the structural differences outlined above, LOXL2-4 are considered a sub-family with separate function from LOX and LOXL1 (Maki 2009). It is well documented that LOX and LOXL1 are important for the organization of the ECM in connective tissues by cross-linking collagen and elastin monomers into insoluble fibers (Lucero and Kagan 2006). Alterations in LOX activity have been associated with numerous diseases including atherogenesis, pulmonary and hepatic fibrosis, and congenital defects such as cutis laxa and the Ehlers-Danlos syndrome (Maki 2009). Recently, demonstration of multiple roles for LOXL proteins in tumorigenesis has led to renewed interest in understanding the biological functions of individual family members (Erler et al. 2009;Levental et al. 2009;Peinado et al. 2005;Peinado et al. 2008;Payne et al. 2007). However, the functional role of most individual LOXL proteins in vertebrate development remains largely unknown.

The zebrafish is an established and powerful model organism for studying the functional roles of proteins during vertebrate embryonic development. This is largely due to the rapid development of the embryo in optically transparent eggs and to the relative ease of genetic manipulation. In recent years, the zebrafish has proven a useful model for elucidating the functional roles of individual lysyl oxidase family members in vertebrate development. Eight zebrafish lysyl oxidase genes have been identified so far encoding for homologs of all human LOXL proteins as well as two additional family members, Loxl5a and Loxl5b (Gansner et al. 2007). Loss of function studies have demonstrated that at least two lysyl oxidases, Loxl1 and Loxl5b, are essential for notochord development (Gansner et al. 2007). In addition, knockdown of *lox* results in subtle notochord defects, neural defects, and abnormal craniofacial development (Reynaud et al. 2008). Chemical inhibition of lysyl oxidases in zebrafish using β-aminopropionitrile and 2-mercaptopyridine-N-oxide results in abnormal craniofacial development that is not entirely explained by the loss of function of Lox (Anderson et al. 2007;Reynaud et al. 2008).

In this investigation we focus on the role of Loxl3 in zebrafish craniofacial development. LOXL3 is highly conserved between humans and rodents and is known to cross-link collagens and elastins *in vitro* (Lee and Kim 2006). A tissue specific LOXL3 splice variant has been identified which has subtle differential affinity for a range of collagens and elastins compared to full-length LOXL3 (Lee and Kim 2006). *LOXL3* expression has been detected in many human adult tissues including cartilage (Huang et al. 2001;Maki and Kivirikko 2001;Jourdan-Le Saux et al. 2001;Sato et al. 2006) while in mid-gestational mice, *Loxl3* was

reported to be exclusively expressed in cartilage (Cankaya et al. 2007). These findings may indicate a functional role for LOXL3 in cartilage development and maintenance.

In zebrafish, two LOXL3 paralogs, Loxl3a and Loxl3b, were previously reported that lacked a signal peptide and functional SRCR domains (Gansner et al. 2007). Zebrafish *loxl3b* is expressed in the notochord from the ten-somite stage while *loxl3a* is not; an analysis of expression after the 20-somite stage was not presented (Gansner et al. 2007). In the present study we report the isolation of full-length *loxl3a* and *loxl3b* cDNAs which are differentially expressed throughout development and demonstrate a critical role for *loxl3b* in craniofacial chondrogenesis.

2. Results

2.1 *loxl3a* and *loxl3b* are orthologs of mammalian *LOXL3*

BLAST searches against the latest version of the zebrafish genomic database (V8) using human *LOXL3* cDNA sequences yielded two zebrafish transcripts with high homology containing full-length SRCR domains in their predicted coding regions. We cloned both genes from an embryonic zebrafish cDNA pool using primers located in the predicted 5′- and 3′-UTRs and identified several transcripts with varying lengths for both genes. The largest *loxl3a* cDNA sequence contained a 2049 bp coding region while the largest *loxl3b* coding region was 2268 bp. Sequencing of the shorter transcripts confirmed that these were *loxl3a* and *loxl3b* splice variants (data not shown). Sequence alignment with human, mouse and rat *Loxl3* cDNA sequences revealed that the longest *loxl3a* and *loxl3b* transcripts were homologous (65% identity) to mammalian *LOXL3* sequences. Alignment of the translated protein sequences revealed some similarity to zebrafish Loxl2a and Loxl2b but phylogenetic analysis clearly demonstrates that they are separate genes (Fig. 1A). Alignment of Loxl3a and Loxl3b protein sequences with human and rodent LOXL3 revealed conservation of the lysyl oxidase domain, lysyl tyrosyl quinone cofactor residues, signal peptide and the SRCR domains (Supplementary Fig. 1), suggesting a conserved molecular function.

2.2 Spatiotemporal expression of *loxl3a* and *loxl3b*

We next investigated the spatiotemporal expression of *loxl3a* and *loxl3b* in the zebrafish embryo from 3 hours post fertilization (hpf) to 120 hpf. Semi quantitative RT-PCR analysis demonstrated that both genes are expressed from 24 hpf until 120 hpf and that *loxl3b* is expressed more abundantly than *loxl3a* at most stages (Fig. 1B). *In situ* hybridization with sequence specific riboprobes revealed that *loxl3b* but not *loxl3a* is expressed within the developing notochord from the 15 somite stage until 30 hpf (Fig. 1C, D and data not shown) which is in concordance with previous findings (Gansner et al. 2007). *loxl3a* is weakly expressed at 30 hpf in the ventral head mesenchyme (Fig. 1C) but not spatially restricted after this time-point (Fig. 1E). *loxl3b* expression appeared in the ventral head mesenchyme at 30 hpf (Fig. 1D) and from 48 hpf, expression was primarily observed within the gut and around the developing craniofacial cartilages including ceratobrachial arches, mandibular and hyoid arches and weakly in the ethmoid plate and trabeculae (Fig. 1F, G, H). The expression of *loxl3b* in the head mesenchyme was maintained until at least 96 hpf. We also performed analysis of 120 hpf embryos but found no expression in the craniofacial cartilages, which was either due to downregulation of expression in these structures or to insufficient penetration of the *loxl3b* riboprobe (data not shown). Together, these findings suggested the possible involvement of *loxl3a* and *loxl3b* in zebrafish craniofacial development between 30 and 96 hpf. Of note, the *in situ* hybridization findings do not reflect relative tissue abundance of the different lysyl oxidase isoforms because the probe characteristics and development times are different.

2.3 Loss of *Loxl3b* but not *Lox3a* leads to craniofacial defects

To examine potential roles of *loxl3a* and *loxl3b* in zebrafish craniofacial development, we injected morpholino antisense oligonucleotides into one- to two-cell stage embryos and monitored development until 120 hpf. Microinjection of a morpholino directed against *loxl3a* did not result in a detectable phenotype at 120 hpf (n>100) (data not shown). To assess the functional role of *loxl3b* in craniofacial development, two non-overlapping splice blocking morpholinos directed at intron-exon boundaries within the lysyl oxidase catalytic domain (MO1 and MO2, Fig. 2A) were injected separately. Injection of either MO1 or MO2 resulted in a similar phenotype at 96 hpf, whereas injection of a general control morpholino at identical doses did not result in any phenotype (Fig. 2B vs. C, D and 2E vs. F, G). Injection of 12 ng of MO1 or 4 ng of MO2 resulted in smaller heads at 72 hpf (data not shown) and micro- or agnathia in approximately 95% of the embryos at 96 hpf (Fig. 2F, G). Alcian blue staining at 120 hpf revealed a reduction of neural crest derived cartilages of the viscerocranium in *loxl3b* morphants which could be categorized into mild and severe phenotypes (Fig. 2H vs. I, J and K). In all morphants, the mandibular and hyoid arch were reduced or misshapen and in severely affected embryos, the ceratobranchial arches were lost entirely (Fig. 2H vs. I, J). The cartilage elements of the neurocranium were impacted to a lesser degree but the ethmoid plate was clearly reduced and the trabeculae were smaller in the most severely affected embryos (Fig.2 J). Importantly, alcian blue staining of embryos injected with control or mismatch morpholinos did not result in any detectable abnormalities (Fig. 2K). RT-PCR analysis using Loxl3b specific primers on single embryos injected with MO1 and MO2, demonstrated that injected embryos were hypomorphic at the morpholino doses employed (Fig. 2L). Despite the specificity of the morphant phenotype, rescue using full-length capped zebrafish *loxl3b* and full-length human *LOXL3* mRNAs was unsuccessful (data not shown). Together, these results demonstrate that partial knockdown of *loxl3b* leads to severe craniofacial abnormalities.

2.4 The *loxl3b* knockdown phenotype is not caused by cell death

One possible explanation for the observed reduction in craniofacial cartilages caused by loss of function of Loxl3b (Fig. 2) could be *p53* mediated cell death caused by morpholino off-targeting (Robu et al. 2007). This was especially relevant since some head necrosis was observed in *loxl3b* morphants (Supplementary Fig. 2). Alternatively, sequence specific knockdown of *loxl3b* could result in cell death since some genes are known to function as survival factors for cranial NCCs (Barrallo-Gimeno et al. 2004). To investigate these possibilities, we injected MO2 into a *p53* deficient background either by co-injection with a morpholino directed at *p53* (P53MO (Robu et al. 2007)) or injection of MO2 into $p53^{-/-}$ embryos (Berghmans et al. 2005). At 24 hpf, co-injection of 4 ng MO2 with 2 ng P53MO or injection of 4 ng MO2 into $p53^{-/-}$ embryos abolished necrosis in the head and hindbrain completely (Supplementary Fig. 2). At 72 hpf head sizes were still somewhat reduced after MO2 injection into a *p53* deficient background (Fig. 3C vs. B, data not shown) which was expected given previous reports on the requirements for craniofacial development and head size (Sperber and Dawid 2008;Baas et al. 2009). Alcian blue staining at 120 hpf consistently demonstrated a severe reduction of craniofacial cartilages when MO2 was injected into both wild type and *p53* deficient embryos (Fig. 3D-I, M, data not shown). Additionally, Acridine orange staining showed no increase in cell death between control embryos and *loxl3b* morphants in a *p53* deficient background (Fig. 3J-L) and no significant cell death within the developing pharyngeal arches at 30 and 48 hpf (Fig. 3K, L, N, O). Together, these results demonstrate that the *loxl3b* craniofacial morphant phenotype is not due to P53 mediated cell death.

2.5 Cartilage elements in *loxl3b* morphant embryos do not mature

To further investigate the timing of the onset of the *loxl3b* morphant phenotype we monitored maturation of cartilage elements from 72 until 96 hpf by staining for glycosylated proteins. Peanut Agglutinin (PNA) and Wheat Germ Agglutinin (WGA) bind glycosylated proteins in the ECM of maturing chondrocytes allowing for early, whole mount analysis of cartilage elements (Fig. 4A, C, E) (Lang et al. 2006;Hall and Miyake 2000). PNA and WGA staining of 72 hpf embryos injected with MO2 revealed a lack of maturing cartilages (Fig. 4B, D). This was not likely to be due to developmental delay since 96 hpf morphant embryos also did not show maturing cartilage with WGA and PNA stains (Fig. 4F, data not shown). These data demonstrated that cartilage elements in *loxl3b* morphant embryos do not mature properly.

2.6 Chondrocyte morphology and ECM are affected by loss of loxl3b function

To further characterize the maturing cartilages of the viscerocranium after loss of function of Loxl3b, we performed histological and ultrastructural analysis on sections of 72 to 120 hpf controlMO and MO2 injected embryos. At 120 hpf, toluidine blue staining on sections of controlMO injected larvae demonstrated the presence of cartilage formation in the ceratohyoid and ceratobranchial arches 1 to 5 (Fig. 5A). In larvae that were injected with 2 ng of MO2 we found that cartilage in ceratobranchial arch 1 and the ceratohyoid was present but had not formed in arches 3-5 in a majority of the embryos (Fig. 5B), providing further support for our initial findings (Fig. 2). Higher magnification of the ceratohyoid at 96 hpf revealed that chondrocyte stacking was disrupted in morphant embryos while overall toluidine blue staining within ceratobranchial arch 1 and 2 was low (Fig. 5C vs. D). We next investigated chondrocyte morphology and ECM with transmission electron microscopy (TEM). In 72 hpf controlMO injected embryos the ceratobranchial arches contain well organized chondrocyte stacks that deposited an ECM containing thin fibrils and proteoglycans (Fig. 5E, F). In 72 hpf, *loxl3b* morphant embryos, chondrocyte organization seemed somewhat disrupted but we found no clear difference in organization of the ECM (Fig 5G, H). At 120 hpf, chondrocytes in control larvae were clearly hypertrophic whereas chondrocytes in *loxl3b* morphants were not (Fig. 5I vs. K). The ECM of chondrocytes in 120 hpf control larvae contained less fibrils when compared to earlier stages but increased amounts proteoglycans (Fig. 5J) which is in accordance with previous findings (Baas et al, 2009). In 120 hpf *loxl3b* morphant embryos, the chondrocyte ECM contained more and abnormally thick fibrils but less proteoglycans (Fig. 5L). The periphery of the 120 hpf control chondrocyte ECM contained a granular layer that seemed to be absent in morphant cartilages (Fig 5I, J vs. K, L). Together, these data indicate that cartilage elements in *loxl3b* morphant embryos do not mature properly and that chondrocyte morphology and ECM is affected by loss of Loxl3b function.

2.7 Differentiation and condensation but not early patterning is affected in *loxl3b* morphants

To gain further insight in the timing and molecular events underlying abnormal craniofacial development in *loxl3b* morphants, we performed *in situ* hybridization with markers for specific events in craniofacial development. Since the affected cartilages were mainly neural crest derived and human LOXL3 is associated with the control of epithelial to mesenchymal transitions (EMT; Peinado et al. 2005) we first examined whether cranial NCCs migrated from the neural fold into the putative pharyngeal arches. We injected 4 ng of MO2 and 2 ng of P53MO into wild-type embryos and used a riboprobe against *sox10*, a marker for migrating NCCs (Dutton et al. 2001). At 22 hpf, NCCs had migrated laterally from the dorsal midline in both P53MO and MO2 injected embryos (Fig. 6A, B) and we obtained identical results using a riboprobe against *crestin*, an alternative marker for migrating NCCs (Luo et al. 2001, data not shown). At 28 hpf, around the time when cranial NCCs have

finished migrating and are populating the pharyngeal arches, we found no difference between P53MO control and MO2/P53MO co-injected embryos in the expression of *dlx2a*, a marker for migratory and post-migratory cranial NCCs (Akimenko et al. 1994) (Fig. 6C, D). These data corroborated our initial finding that the pharyngeal arches form normally in *loxl3b* morphants (Fig. 3N, O). In addition, in *loxl3b* morphants, expression of *hand2*, an essential factor for ventral arch specification expressed in a ventrally located subset of NCC in the pharyngeal arches (Miller et al., 2000), showed no difference at 36 hpf (Fig. 6E, F). However, at 48 hpf *loxl3b* morphant embryos showed perturbed expression of the chondrogenic differentiation marker *sox9a* (Fig. 6G vs. H) and its direct downstream target *col2a1* (Fig. 6I vs. J). This unlikely to be due to developmental delay since both markers were still not expressed in the ceratobranchial arches in morphant embryos at 72 hpf (data not shown). Importantly, expression of *gsc*, a marker for hyoid condensation (Schulte-Merker et al. 1994) was also perturbed (Fig. 6L vs. K). Taken together, these findings show that initial patterning of the pharyngeal arches in *loxl3b* morphants is normal whereas differentiation is impaired and suggest that this could be due to improper chondrogenic progenitor cell condensation.

2.8 proliferation of chondrogenic progenitor cells is reduced in *loxl3b* morphants

Between 30 and 48 hpf there is considerable outgrowth of the pharyngeal arches in the anterior direction. During this phase chondrogenic progenitor cells condense and go through a highly proliferative phase (Sperber and Dawid 2008;Goldring et al. 2006;Hall and Miyake 2000). Since initial patterning of the arches was normal and the phenotype could not be explained by P53 mediated cell death, we investigated whether chondrogenic progenitor cells within the pharyngeal arches were proliferating at comparable rates in control injected and *loxl3b* morphant embryos. We used the *sox10:rfp* transgenic line in which the neural crest derived chondrogenic progenitor cells are labeled with a membrane bound red fluorescent protein, in combination with a phosphohistone H3 (phosphoH3) antibody, which labels nuclei of proliferating cells. This allowed us to determine the number of proliferating neural crest derived chondrogenic progenitor cells within the pharyngeal arch condensations. We found that *loxl3b* morphant embryos had a severely reduced number of phosphoH3 labeled nuclei at 36 hpf (Fig. 7A, B) and quantification of the number of proliferating cells within the arches confirmed these findings (Fig. 7C). These data demonstrated that cell proliferation of chondrogenic progenitor cells was reduced in *loxl3b* morphant embryos at 36 hpf (n>3).

3. Discussion

Here we report the identification of two full-length zebrafish orthologs of mammalian LOXL3. We show that *loxl3a* and *loxl3b* are differentially expressed during zebrafish development and that *loxl3b* is abundantly expressed in head mesenchyme and developing cartilages that will form the zebrafish craniofacial skeleton (Fig. 1). Using a loss of function approach and analysis of craniofacial chondrogenesis, we provide evidence for a role of Loxl3b in proliferation and differentiation of chondrogenic progenitor cells. This is the first report of the involvement of this lysyl oxidase protein in craniofacial chondrogenesis.

There are multiple lines of evidence presented in this study that demonstrate a gene specific phenotype. First, the two independent *lox3b* morpholinos used in this study showed similar phenotypes (Fig. 2) while RT-PCR analysis confirmed that the injected embryos were hypomorphic for *loxl3b* at doses that caused disruption of craniofacial development (Fig. 2). Furthermore, injection of a general control morpholino and a 5-mismatch morpholino for MO2 up to 12 ng did not result in a detectable phenotype. While we were unable to rescue the morphant phenotype with full length zebrafish *loxl3b* or human *LOXL3* capped mRNA, this finding is not uncommon for proteins with functions in the extracellular compartment

(Baas et al. 2009) and may be attributed to a non-physiologic distribution of the injected mRNA or to its degradation, especially in view of the late time window in which Loxl3b functions. It is also possible that alternatively spliced transcripts are required within pharyngeal arch condensations for proper cartilage maturation. Consistent with this hypothesis, a tissue specific splice variant of *LOXL3* is known to have differential affinity for collagen and elastin monomers (Lee and Kim 2006), and as noted above, we found several splice variants of *loxl3b*, similar to what has been reported for humans and rodents (Maki 2009). Given the specificity of the *loxl3b* morphant phenotype, and the concordance of the phenotype with *loxl3b* expression in head mesenchyme, the data presented here demonstrate that *loxl3b* is critical for zebrafish craniofacial development.

The full-length zebrafish Loxl3a and Loxl3b proteins contain a signal peptide and scavenger receptor cysteine-rich (SRCR) domains in the N-terminal region in addition to a functional lysyl oxidase domain in the C-terminal region (Supplementary Fig. 1). Conservation of these domains between mammals and zebrafish suggests a role for Loxl3b in organizing the ECM. The conservation of a signal peptide in both proteins suggests that they are secreted providing additional support for this idea. It is worth noting that human LOXL3 is secreted in cell culture systems and can cross-link collagen type II *in vitro* (Lee and Kim 2006). These reports raise the possibility that *loxl3b* is required for ECM organization in chondrogenic progenitor condensations which may be critical for chondrogenesis. Although a role for Loxl3b in the extracellular compartment seems likely, it is interesting to note that SRCR domains are found in membrane-associated proteins involved in cell adhesion and signal transduction (Yamada et al. 1998). In addition, several studies have shown the intracellular localization of LOXL3 (Lee and Kim 2006;Peinado et al. 2005) and other members of the lysyl oxidase protein family are known to have intracellular functions (Maki 2009). It is therefore possible that Loxl3b may function in the intra- or extracellular compartment or both.

Condensation of chondrogenic progenitor cells is essential for the development of vertebrate craniofacial cartilages (Hall and Miyake 2000). Although this process is not entirely understood, proliferation and differentiation within mesenchymal condensations are dependent on cell-ECM interactions (Woods et al. 2007). Therefore, the integrity of the ECM within the pharyngeal arches is likely to be important for chondrogenic progenitor cell proliferation and differentiation. It is well established that inhibition of lysyl oxidase activity or morpholino mediated knockdown of specific lysyl oxidase family members compromises the integrity of the ECM which leads to aberrant morphogenesis in zebrafish (Gansner et al. 2007;Anderson et al. 2007;van Boxtel et al. 2010). Furthermore, there are several reports that directly implicate lysyl oxidases in cellular proliferation (Maki 2009;Di Donato A. et al. 1997). Evidence for a role of LOXL3 in proliferation of chondrogenic cells comes from a comparison of gene expression profiles between healthy and damaged cartilage in which hierarchical clustering revealed an association between LOXL3 expression and the expression of proliferation associated genes (Sato et al. 2006). Recent research has shown that matrix cross-linking by LOX leads to enhanced integrin signaling in tumor cells (Levental et al. 2009). Individual lysyl oxidases may therefore be important for organizing the ECM, necessary for chondrogenesis.

Our histological and ultrastructural analysis of cartilage elements in Loxl3b deficient embryos revealed that chondrocyte organization and morphology is abnormal (Fig 5). The observed abnormalities are reminiscent of loss of ECM integrity such as caused by the loss of Col11a1 function (Baas et al, 2009). Given the plausible role of Loxl3b in cross-linking collagens in the ECM of chondrogenic condensations, we expected to find less fibrils in the ECM surrounding chondrocytes in 72 hpf Loxl3b morphant embryos. However, we found no evidence for this but instead found that in 120 hpf loxl3b morphant embryos, more and

thicker fibrils were present in chondrocyte ECM (Fig 5). This could be explained by compensatory mechanisms or by morpholino degradation and dilution at later stages. Recent research suggests that craniofacial chondrogenesis is dependent on sensing the formation of a properly organized ECM, in part established by cross-linking by lysyl oxidases (Mangos et al. 2010). A sensory mechanism involving polcystine (Pkd) 1a, Pkd1b and Pkd2 was shown to play a vital role in the transcriptional control structural proteins including proteins, necessary for chondrogenesis. Such a mechanism may provide a basis for further understanding the interaction between differentiating chondrogenic progenitor cells and organization of the ECM by lysyl oxidases (Mangos et al. 2010). The zebrafish will provide an excellent model organism to further investigate these interactions *in vivo*.

Together, the data presented in this report provide evidence for a novel and exciting role for *loxl3b* in chondrogenesis during zebrafish craniofacial development. In addition, a previous report has indicated that *lox* may also be involved in zebrafish craniofacial development (Reynaud et al. 2008). Since there are ten lysyl oxidases in zebrafish (Gansner et al, 2007 and unpublished data) there may be more lysyl oxidases needed for chondrogenesis. Although there are currently no known mutations in LOXL3 that lead to craniofacial pathogenesis, these findings should be placed in the context of the complex interplay between nutritional status, genetic variation and environmental factors that contribute to craniofacial pathogenesis (Gansner et al. 2007). Further studies into the precise molecular role of Loxl3b will lead to a better understanding of the genetic and environmental factors that contribute to craniofacial pathogenesis.

4. Experimental procedures

4.1 Animal care and transgenic zebrafish

Wild-type (AB), Tg(*sox10(7.2):mrfp*)^{vu234} (Kirby et al. 2006) and *tp53*$^{-/-}$ fish (Berghmans et al. 2005) were maintained under standard conditions and embryos were isolated as previously described (Westerfield 2000). Embryos and larvae were staged as previously described (Kimmel et al. 1995) and fixed in 4% paraformaldehyde (PFA), dehydrated in methanol and stored at -20°C for further analysis.

4.2 RT-PCR and cloning

Loxl3a and *loxl3b* were cloned by RT-PCR using RNA from staged, pooled wild-type embryos. Briefly, RNA was isolated using Trizol reagent (Invitrogen, The Netherlands) and reverse transcription was performed using 0.5 μg of total RNA and a High Capacity cDNA Reverse Transcriptase Kit (Applied Biosystems, The Netherlands). The following primers were used: *loxl3a* fw: 5′-CCTTAACCGACTGTCAGCATCATTC-3′; *loxl3a* rv: 5′-GCATTCAGCACTAGATCCGAAGC-3′; *loxl3b* fw: 5′-TTGGATTCCATCATGCTTTG-3′; *loxl3b* rv: 5′-AGCCCATCCGTCCTTATTCT-3′. The primer annealing temperature was 58°C and 30 cycles of PCR were performed. Full-length *loxl3a* and *loxl3b* clones were then generated by nested (*loxl3a*) or direct (*loxl3b*) PCR using Phusion DNA polymerase (Finnzymes, Finland) and the following primers: *loxl3a* 5′UTR fw: 5′-TTCATCTCTCACACTTTGAAGCCATGC-3′; *loxl3a* 3′UTR rv: 5′-CAGAGCCACGCTGTTGTTGCG-3′; *loxl3a* fw: 5′-CTGGATCCGCCATGCTGAGAAGTGAACTTAGGG-3′; *loxl3a* rv: 5′-CTCTCGAGTGAGATCTTGTTGTTGAGCTGCCC-3′; *loxl3b* fw: 5′-CTGGATCCCACATGGAGCTGCATCAATGGTG-3′; *loxl3b* rv: 5′-TGGAATTCTGAGATCTGGTTGTTCAGTTGTCCAG-3′. The PCR products were digested with BamHI/EcoRI (NEB, The Netherlands), purified using a PCR product purification kit (Qiagen, The Netherlands) and cloned into the BamHI/EcoRI digested pcDNA3.1-V5-HisA plasmid (Invitrogen, The Netherlands). At least three independent

clones were sequenced with at least double coverage and alignments were performed with ClustalW2.

4.3 Cartilage and glycosylated protein staining

For analysis of cartilage elements, 120 hours post fertilization (hpf) larvae were fixed for 30 min at room temperature in 4% PFA and stained overnight in 0.1% Alcian blue in 70% ethanol, 5% hydrochloric acid. Next, the embryos were extensively washed in 70% ethanol, 5% hydrochloric acid. The larvae were cleared in 50% glycerol, 2 mM potassium hydroxide and mounted on microscopy slides using Eukitt mounting medium (Fluka, The Netherlands) for imaging. Percentage effect on craniofacial development was determined by scoring the number of embryos with craniofacial defects after Alcian Blue staining as the fraction of the total number of injected embryos under a stereomicroscope.

Maturation of cartilage elements was visualized by peanut agglutinin (PNA) and wheat germ agglutinin (WGA) that selectively recognize glycosylated proteins in maturing cartilage (Lang et al. 2006). Embryos were fixed at 72 and 96 hpf and labeled whole mount with peanut agglutinin (1:500; Vector Laboratories, USA) or wheat germ agglutinin (1:2500; Vector Laboratories, USA). Photographs were taken under a stereomicroscope equipped with a digital camera (Leica, The Netherlands) and the number of affected larvae was scored.

4.4 Morpholino injections

Morpholino oligonucleotides (Nasevicius and Ekker 2000) targeting the translation start site or splice sites of exons in the *loxl3b* or *tp53* genes were resuspended in double distilled water, diluted to include 0.05% phenol red, and injected into one- to two-cell stage embryos with a microinjection pump (Picopump, Harvard Apparatus, USA) under a stereomicroscope (Leica, USA). Morpholino sequences were: MO1: 5′-AGTGTATGTTTACCCGTGACATGCG-3′; MO2: 5′-GATCTGGAGCAGCTAGAAAAAACAA-3′; mismatch (mm)MO2: 5′-CAGGTGCGCACATTAACATACATAT-3′; P53MO: 5′-GCGCCATTGCTTTGCAAGAATTG-3′ (Robu et al. 2007); standard control MO: 5′-CCTCTTACCTCAGTTACAATTTATA-3′. Efficiency of the *loxl3b* splice morpholinos was measured using RT-PCR on RNA isolated from single embryos with Trizol (Invitrogen, The Netherlands). *Loxl3b* primers spanning intron-exon boundaries were used: *loxl3b* fw: 5′-ACCATGGCCTACAAGAAACG-3′; *loxl3b* rv: 5′-GTCATGCCGATACAAATCCC-3′. Elongation factor 1α (*ef1α*) was amplified as an internal control using the following primers: *ef1α* fw: 5′-CTTCTCAGGCTGACTGTGC-3′; *ef1α* rv: 5′-CCGCTAGCATTACCCTCC-3′. The efficiency and the characterisation of the *p53* morpholino is described elsewhere (Robu et al. 2007). Percentage effect on craniofacial development was determined by scoring the number of embryos with craniofacial defects after alcian blue staining as a fraction of the total number of injected embryos under a stereomicroscope.

4.5 Histology and transmission electron microscopy

For histological and ultrastructural analysis, embryos injected with 2 ng controlMO or 2 ng MO2 were fixed at indicated time-points in 2.5% glutaraldehyde, postfixed with 1% osmium tetroxide, dehydrated in ethanol, infiltrated with propylene oxide and embedded in Epon Resin (Polysciences, USA). Sections were stained with toluidine blue (Sigma Aldrich, The Netherlands) and examined under a phase contrast microscope (Olympus XC31, The Netherlands) mounted with a digital camera (Altra 20, Olympus, the Netherlands) to determine distortions in craniofacial development. Ultrathin sections were stained with uranyl acetate and lead citrate and examined with a transmission electron microscope (JEOL 1010). At least three embryos were examined for each condition.

4.6 In situ hybridization

DIG-labeled antisense RNA probes were synthesized using a DIG-labeling kit (Roche, The Netherlands) and the following constructs: *loxl3a, loxl3b* (Gansner et al. 2007), *col2a1* (Yan et al. 1995), *sox9a* (Yan et al. 2002), *sox10* (Dutton et al. 2001), *dlx2a* (Akimenko et al. 1994), *hand2 (*Angelo et al. 2000*), goosecoid* (Schülte-Merker et al. 1994) and *crestin* (Luo et al. 2001). Whole mount *in situ* hybridization was performed as previously described (Thisse et al. 1993). Embryos were either directly photographed in phosphate-buffered saline (PBS) containing ethylenediaminetetraacetic acid (EDTA) or dehydrated in methanol and cleared and photographed in 1:2 benzyl alcohol: benzyl benzoate.

4.7 Proliferation assay

Embryos and larvae were fixed in 4% PFA, 8% sucrose in PBS overnight at 4°C. Embryos were then embedded in agar (1.5% agarose, 5% sucrose in double distilled water) and incubated in 30% sucrose overnight. 10 μm sections were cut on a Cryostat (Leica, USA) and transferred to Superfrost Plus slides (VWR, USA). Next, sections were rehydrated in PBS for 60 min at room temperature and blocked in 2% goat serum, 2% bovine serum albumin in PBS for 30 min. Incubation with primary rabbit Phospho-Histone H3 antibody (1:1000; Upstate Biotechnology, USA) was performed overnight at 4°C after which sections were rinsed with PBS, incubated for 3 h at 23°C with goat anti-rabbit Alexa Fluor 647 secondary antibodies (Molecular Probes, USA) and rinsed in PBS for 45 min. Sections were mounted in Vectashield (Vector Laboratories, USA) and images were captured using a 40X oil-immersion objective mounted on a motorized microscope (Axiovert 200, Zeiss, USA) equipped with an ERS spinning-disk confocal system (PerkinElmer, USA). Sections of at least 3 embryos were inspected per treatment and cell numbers were counted manually.

Supplementary Material

Refer to Web version on PubMed Central for supplementary material.

Acknowledgments

We thank Prof. M. Westerfield for the *dlx2* and *sox9a* plasmids, Dr. S. Kucenas for the *sox10* plasmid and Dr. E. Knapik for help with PNA and WGA staining. J. Wortel, R. Dekker and Dr. H. de Wit are acknowledged for their aid in histological and TEM analysis. Grant Sponsors: National Institutes of Health DK 44464 (JDG) and T32 GM07200 (JMG), the Netherlands Genomics Initiative (NGI/Ecogenomics) and Netherlands Organization for Scientific Research (864.09.005).

References

Akimenko MA, Ekker M, Wegner J, Lin W, Westerfield M. Combinatorial expression of three zebrafish genes related to distal-less: part of a homeobox gene code for the head. J Neurosci. 1994; 14:3475–3486. [PubMed: 7911517]

Anderson C, Bartlett SJ, Gansner JM, Wilson D, He L, Gitlin JD, Kelsh RN, Dowden J. Chemical genetics suggests a critical role for lysyl oxidase in zebrafish notochord morphogenesis. Mol Biosyst. 2007; 3:51–59. [PubMed: 17216056]

Angelo S, Lohr J, Lee KH, Ticho BS, Breitbart RE, Hill S, Yost HJ, Srivastava D. Conservation of sequence and expression of Xenopus and zebrafish dHAND during cardiac, branchial arch and lateral mesoderm development. Mech Dev. 2000; 95:231–7. [PubMed: 10906469]

Baas D, Malbouyres M, Haftek-Terreau Z, Le GD, Ruggiero F. Craniofacial cartilage morphogenesis requires zebrafish col11a1 activity. Matrix Biol. 2009a; 28:490–502. [PubMed: 19638309]

Barrallo-Gimeno A, Holzschuh J, Driever W, Knapik EW. Neural crest survival and differentiation in zebrafish depends on mont blanc/tfap2a gene function. Development. 2004; 131:1463–1477. [PubMed: 14985255]

Berghmans S, Murphey RD, Wienholds E, Neuberg D, Kutok JL, Fletcher CD, Morris JP, Liu TX, Schulte-Merker S, Kanki JP, Plasterk R, Zon LI, Look AT. tp53 mutant zebrafish develop malignant peripheral nerve sheath tumors. Proc Natl Acad Sci U S A. 2005; 102:407–412. [PubMed: 15630097]

Cankaya M, Hernandez AM, Ciftci M, Beydemir S, Ozdemir H, Budak H, Gulcin I, Comakli V, Emircupani T, Ekinci D, Kuzu M, Jiang Q, Eichele G, Kufrevioglu OI. An analysis of expression patterns of genes encoding proteins with catalytic activities. BMC Genomics. 2007; 8:232. [PubMed: 17626619]

Di Donato A, Lacal JC, Di DM, Giampuzzi M, Ghiggeri G, Gusmano R. Micro-injection of recombinant lysyl oxidase blocks oncogenic p21-Ha-Ras and progesterone effects on Xenopus laevis oocyte maturation. FEBS Lett. 1997; 419:63–68. [PubMed: 9426221]

Dutton KA, Pauliny A, Lopes SS, Elworthy S, Carney TJ, Rauch J, Geisler R, Haffter P, Kelsh RN. Zebrafish colourless encodes sox10 and specifies non-ectomesenchymal neural crest fates. Development. 2001; 128:4113–4125. [PubMed: 11684650]

Erler JT, Bennewith KL, Cox TR, Lang G, Bird D, Koong A, Le QT, Giaccia AJ. Hypoxia-induced lysyl oxidase is a critical mediator of bone marrow cell recruitment to form the premetastatic niche. Cancer Cell. 2009; 15:35–44. [PubMed: 19111879]

Gansner JM, Mendelsohn BA, Hultman KA, Johnson SL, Gitlin JD. Essential role of lysyl oxidases in notochord development. Dev Biol. 2007; 307:202–213. [PubMed: 17543297]

Goldring MB, Tsuchimochi K, Ijiri K. The control of chondrogenesis. J Cell Biochem. 2006; 97:33–44. [PubMed: 16215986]

Hall BK, Miyake T. All for one and one for all: condensations and the initiation of skeletal development. Bioessays. 2000; 22:138–147. [PubMed: 10655033]

Helms JA, Schneider RA. Cranial skeletal biology. Nature. 2003; 423:326–331. [PubMed: 12748650]

Huang Y, Dai J, Tang R, Zhao W, Zhou Z, Wang W, Ying K, Xie Y, Mao Y. Cloning and characterization of a human lysyl oxidase-like 3 gene (hLOXL3). Matrix Biol. 2001; 20:153–157. [PubMed: 11334717]

Jourdan-Le Saux C, Tomsche A, Ujfalusi A, Jia L, Csiszar K. Central nervous system, uterus, heart, and leukocyte expression of the LOXL3 gene, encoding a novel lysyl oxidase-like protein. Genomics. 2001; 74:211–218. [PubMed: 11386757]

Kimmel CB, Ballard WW, Kimmel SR, Ullmann B, Schilling TF. Stages of embryonic development of the zebrafish. Dev Dyn. 1995; 203:253–310. [PubMed: 8589427]

Kirby BB, Takada N, Latimer AJ, Shin J, Carney TJ, Kelsh RN, Appel B. In vivo time-lapse imaging shows dynamic oligodendrocyte progenitor behavior during zebrafish development. Nat Neurosci. 2006; 9:1506–1511. [PubMed: 17099706]

Lang MR, Lapierre LA, Frotscher M, Goldenring JR, Knapik EW. Secretory COPII coat component Sec23a is essential for craniofacial chondrocyte maturation. Nat Genet. 2006; 38:1198–1203. [PubMed: 16980978]

Lee JE, Kim Y. A tissue-specific variant of the human lysyl oxidase-like protein 3 (LOXL3) functions as an amine oxidase with substrate specificity. J Biol Chem. 2006; 281:37282–37290. [PubMed: 17018530]

Levental KR, Yu H, Kass L, Lakins JN, Egeblad M, Erler JT, Fong SF, Csiszar K, Giaccia A, Weninger W, Yamauchi M, Gasser DL, Weaver VM. Matrix crosslinking forces tumor progression by enhancing integrin signaling. Cell. 2009; 139:891–906. [PubMed: 19931152]

Lucero HA, Kagan HM. Lysyl oxidase: an oxidative enzyme and effector of cell function. Cell Mol Life Sci. 2006; 63:2304–2316. [PubMed: 16909208]

Luo R, An M, Arduini BL, Henion PD. Specific pan-neural crest expression of zebrafish Crestin throughout embryonic development. Dev Dyn. 2001; 220:169–174. [PubMed: 11169850]

Mangos S, Lam PY, Zhao A, Liu Y, Mudumana S, Vasilyev A, Liu A, Drummond IA. The ADPKD genes pkd1a/b and pkd2 regulate extracellular matrix formation. Dis Model Mech. 2010; 3:354–65. [PubMed: 20335443]

Maki JM. Lysyl oxidases in mammalian development and certain pathological conditions. Histol Histopathol. 2009; 24:651–660. [PubMed: 19283672]

Maki JM, Kivirikko KI. Cloning and characterization of a fourth human lysyl oxidase isoenzyme. Biochem J. 2001; 355:381–387. [PubMed: 11284725]

Nasevicius A, Ekker SC. Effective targeted gene 'knockdown' in zebrafish. Nat Genet. 2000; 26:216–220. [PubMed: 11017081]

Payne SL, Hendrix MJ, Kirschmann DA. Paradoxical roles for lysyl oxidases in cancer-a prospect. J Cell Biochem. 2007; 101:1338–1354. [PubMed: 17471532]

Peinado H, Del Carmen Iglesias-de la Cruz, Olmeda D, Csiszar K, Fong KS, Vega S, Nieto MA, Cano A, Portillo F. A molecular role for lysyl oxidase-like 2 enzyme in snail regulation and tumor progression. EMBO J. 2005; 24:3446–3458. [PubMed: 16096638]

Peinado H, Moreno-Bueno G, Hardisson D, Perez-Gomez E, Santos V, Mendiola M, de Diego JI, Nistal M, Quintanilla M, Portillo F, Cano A. Lysyl oxidase-like 2 as a new poor prognosis marker of squamous cell carcinomas. Cancer Res. 2008; 68:4541–4550. [PubMed: 18559498]

Reynaud C, Baas D, Gleyzal C, Le GD, Sommer P. Morpholino knockdown of lysyl oxidase impairs zebrafish development, and reflects some aspects of copper metabolism disorders. Matrix Biol. 2008; 27:547–560. [PubMed: 18467084]

Robu ME, Larson JD, Nasevicius A, Beiraghi S, Brenner C, Farber SA, Ekker SC. p53 activation by knockdown technologies. PLoS Genet. 2007; 3:e78. [PubMed: 17530925]

Sato T, Konomi K, Yamasaki S, Aratani S, Tsuchimochi K, Yokouchi M, Masuko-Hongo K, Yagishita N, Nakamura H, Komiya S, Beppu M, Aoki H, Nishioka K, Nakajima T. Comparative analysis of gene expression profiles in intact and damaged regions of human osteoarthritic cartilage. Arthritis Rheum. 2006; 54:808–817. [PubMed: 16508957]

Schulte-Merker S, Hammerschmidt M, Beuchle D, Cho KW, De Robertis EM, Nusslein-Volhard C. Expression of zebrafish goosecoid and no tail gene products in wild-type and mutant no tail embryos. Development. 1994; 120:843–852. [PubMed: 7600961]

Sperber SM, Dawid IB. barx1 is necessary for ectomesenchyme proliferation and osteochondroprogenitor condensation in the zebrafish pharyngeal arches. Dev Biol. 2008; 321:101–110. [PubMed: 18590717]

Szabo-Rogers HL, Smithers LE, Yakob W, Liu KJ. New directions in craniofacial morphogenesis. Dev Biol. 2010; 341:84–94. [PubMed: 19941846]

Thisse C, Thisse B, Schilling TF, Postlethwait JH. Structure of the zebrafish snail1 gene and its expression in wild-type, spadetail and no tail mutant embryos. Development. 1993; 119:1203–1215. [PubMed: 8306883]

van Boxtel AL, Kamstra JH, Fluitsma DM, Legler J. Dithiocarbamates are teratogenic to developing zebrafish through inhibition of lysyl oxidase activity. Toxicol Appl Pharmacol. 2010; 244:156–61. [PubMed: 20045017]

Westerfield, M. The zebrafish book. Eugene, Oregon: University of Oregon Press; 2000.

Woods A, Wang G, Beier F. Regulation of chondrocyte differentiation by the actin cytoskeleton and adhesive interactions. J Cell Physiol. 2007; 213:1–8. [PubMed: 17492773]

Yamada Y, Doi T, Hamakubo T, Kodama T. Scavenger receptor family proteins: roles for atherosclerosis, host defence and disorders of the central nervous system. Cell Mol Life Sci. 1998; 54:628–640. [PubMed: 9711230]

Yan YL, Hatta K, Riggleman B, Postlethwait JH. Expression of a type II collagen gene in the zebrafish embryonic axis. Dev Dyn. 1995; 203:363–376. [PubMed: 8589433]

Yan YL, Miller CT, Nissen RM, Singer A, Liu D, Kirn A, Draper B, Willoughby J, Morcos PA, Amsterdam A, Chung BC, Westerfield M, Haffter P, Hopkins N, Kimmel C, Postlethwait JH. A zebrafish sox9 gene required for cartilage morphogenesis. Development. 2002; 129:5065–5079. [PubMed: 12397114]

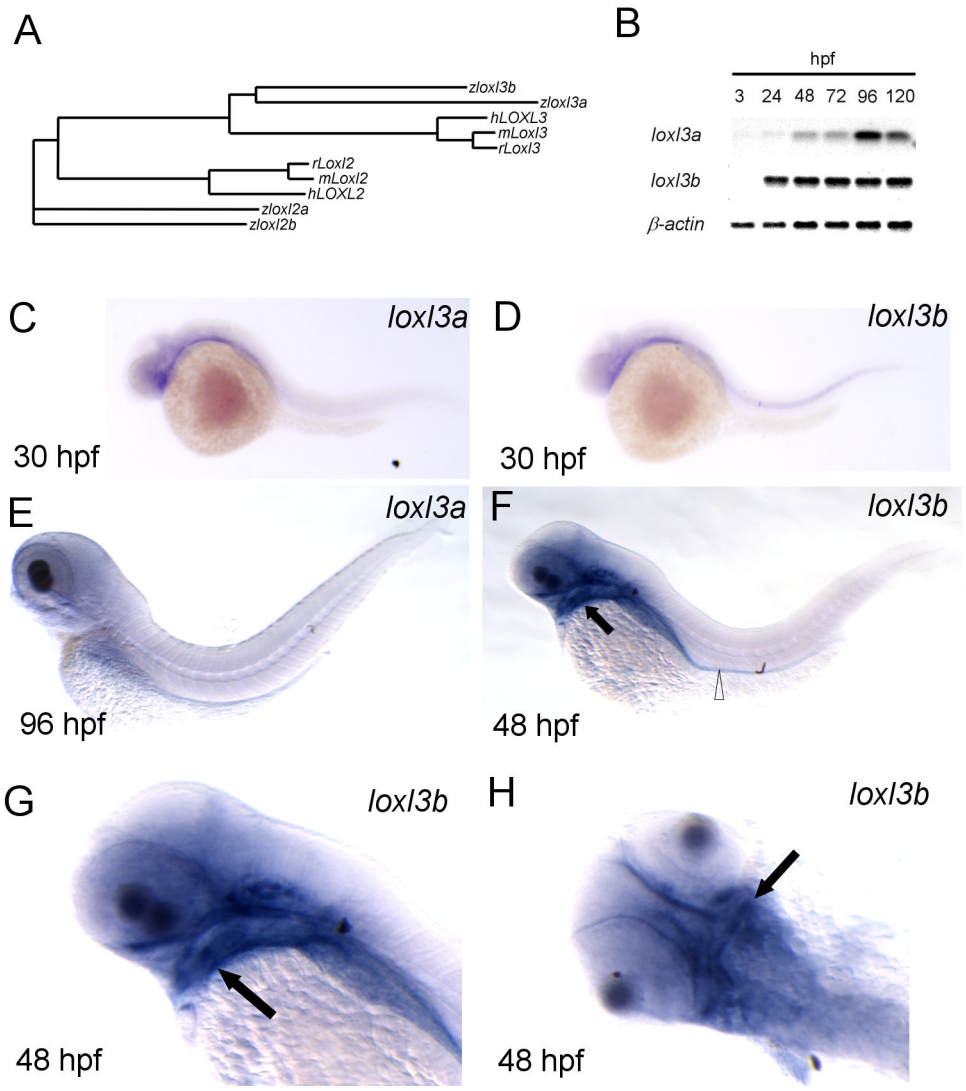

Fig. 1.

Loxl3b is expressed in head mesenchyme and gut. A: Phylogenetic tree based on protein sequences of full-length zebrafish (z) Loxl3a and Loxl3b with human (h) and mouse (m) orthologs. Loxl2 sequences are included for comparison. B: Non-saturated agarose gel images for *loxl3a* and *loxl3b* RT-PCR, using RNA from embryos at the indicated developmental stages. The housekeeping gene *β-actin* was amplified as a control. C-H: Spatiotemporal expression of *loxl3a* and *loxl3b* by *in situ* hybridization at the indicated developmental stages. Note that staining intensity does not reflect expression levels. F, G and H are the same embryo. Open triangle: gut; black arrow: developing cartilage.

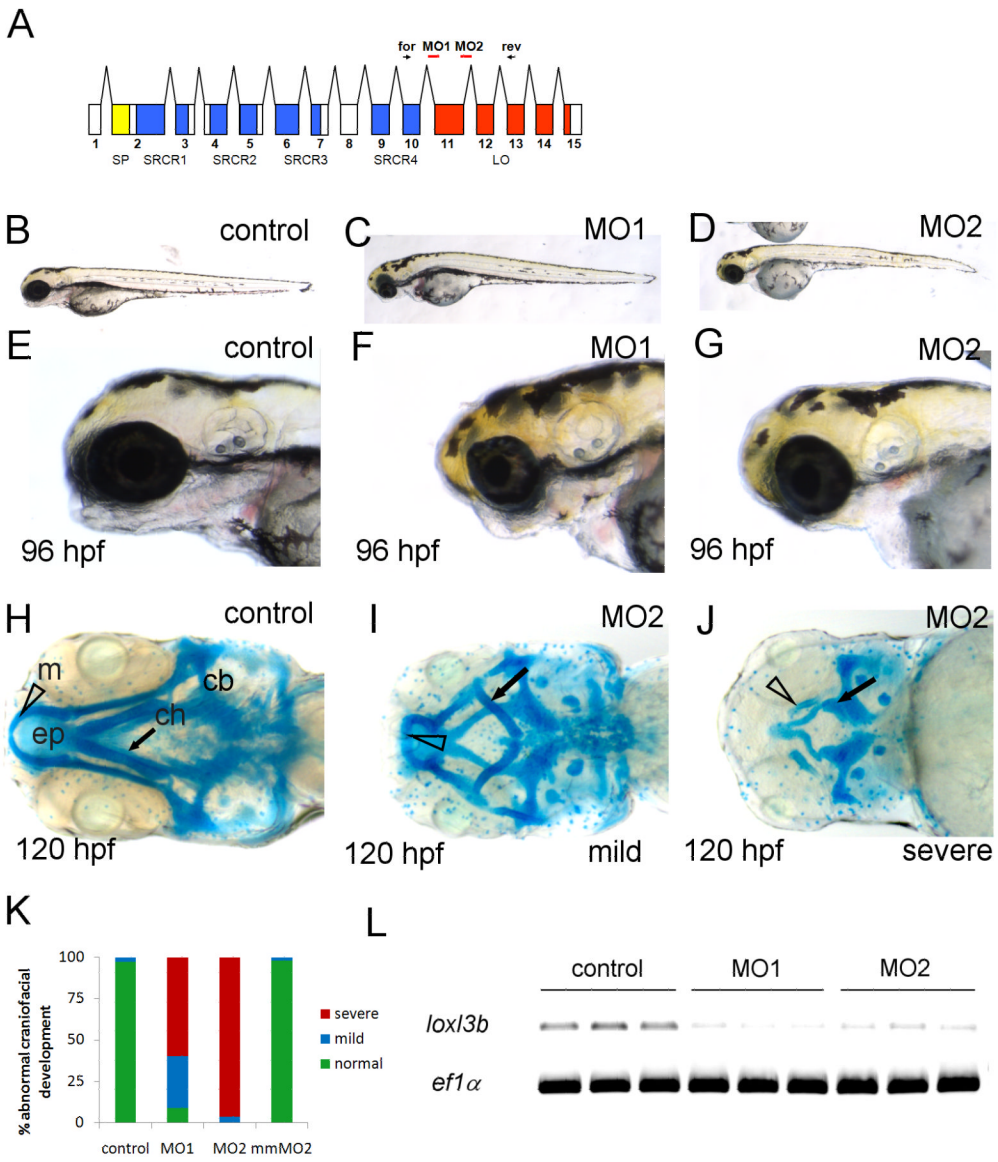

Fig. 2.

Craniofacial cartilage formation is impaired in *loxl3b* morphant embryos. A: Schematic of the *loxl3b* transcript showing the location of sites targeted by morpholinos (red lines) used in this study (MO1 and MO2). Signal peptide (SP) depicted in yellow, scavenger receptor cysteine-rich (SRCR) domains are in blue and the lysyl oxidase (LO) domain is in red. Forward and reverse primers for confirmation of knock down are depicted as arrows (for and rev). B-D: Lateral view of 96 hpf embryos injected with control (B) or MO1 (C) and MO2 (D). E-G: Lateral view of heads of injected with control (E), MO1 (F) or MO2 (G). H-J: Alcian blue staining of 120 hpf embryos injected with control (H) or MO2 (I, J). K: Graph depicting percentages of normal (green) mildly (blue) and severely (red) effected craniofacial development after injection with indicated morpholinos, scored after alcian blue and alazarin red staining (n>100). L: RT-PCR for *loxl3b* in single embryos injected with 20 ng control morpholino or *loxl3b* splice morpholinos (4ng MO1 and 12 ng MO2). Reactions were conducted on triplicate samples, as shown. The housekeeping gene *ef1α* was amplified

as a control. Open triangle, m: mandibular; black arrow, ch: ceratohyoid; cb: ceratobranchial, ep: ethmoid plate.

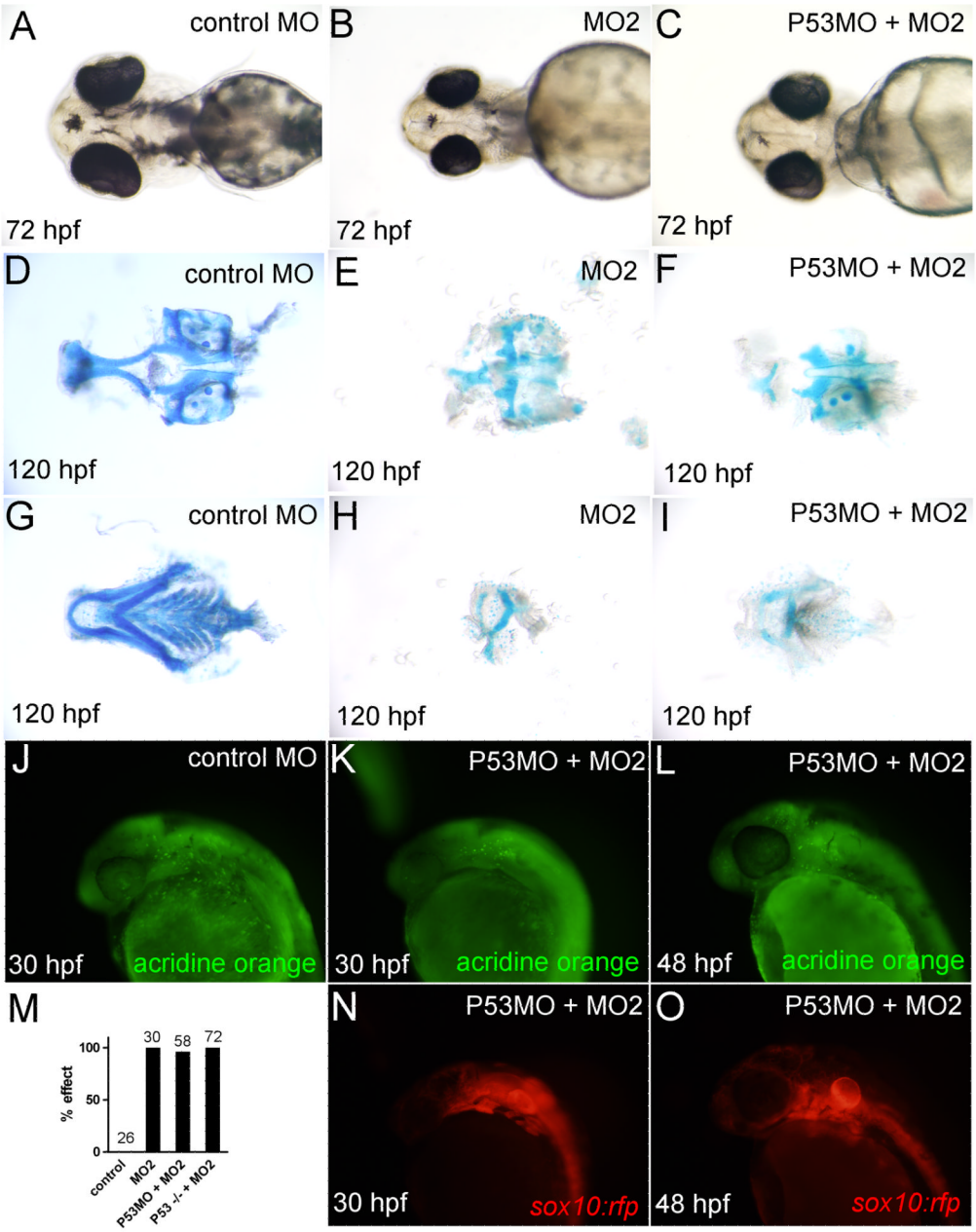

Fig. 3.

The *loxl3b* morphant phenotype is not caused by *p53*-mediated cell death. A-C: Light microscopic images of 72 hpf embryos injected with control (A), 4 ng MO2 (B), or 2 ng P53MO and 4 ng MO2 (C) morpholino. D-F: Alcian blue staining of ventral cartilages from 72 hpf embryos injected with control (D), MO2 (E), or P53MO and MO2 (F). G-I: Alcian blue staining of dorsal cartilages from 120 hpf embryos injected with control (G), MO2 (H), or P53MO and MO2(I). J-L: Acridine orange staining in 30 and 48 hpf embryos in control (J) and P53MO and MO2 injected embryos (K, L). Corresponding images of *sox10:rfp* embryos are included for comparison (N, O). M: Quantification of number of affected embryos in wild-type and $p53^{-/-}$ embryos injected with control, MO2 or P53MO.

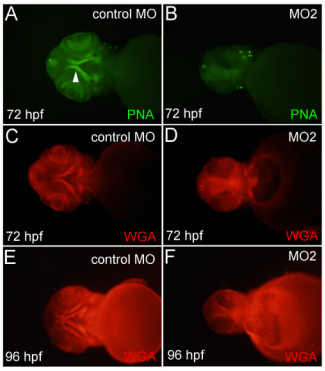

Fig. 4.

Cartilage fails to mature in *loxl3b* morphants. Images of control injected embryos (A, C, E) or fish injected with 4 ng MO2 morpholino (B, D, F) stained for glycosylated proteins with peanut agglutinin (PNA) and wheat germ agglutinin (WGA) and imaged at 72 and 96 hpf. White triangle: maturing cartilage.

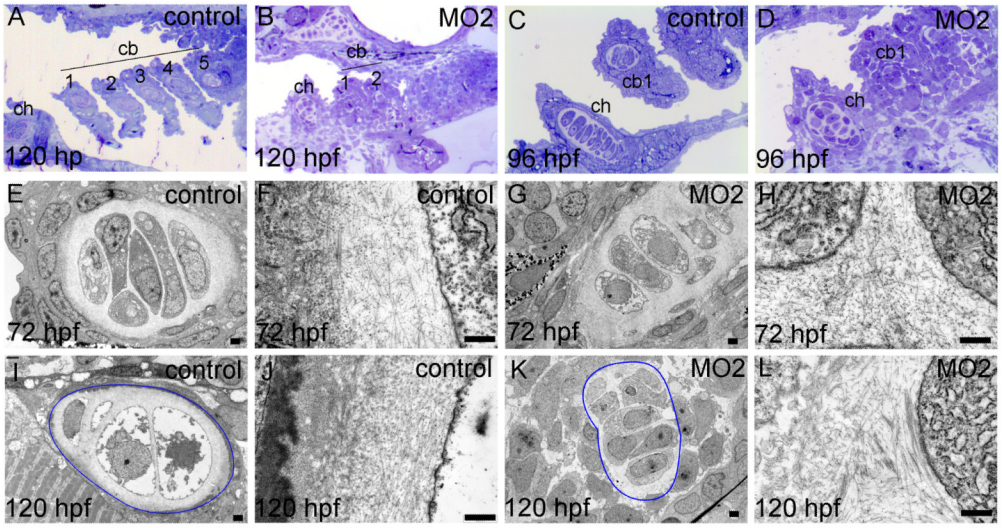

Fig. 5.

Chondrocyte morphology, stacking and ECM are abnormal in *loxl3b* morphants. Zebrafish embryos were injected with 2 ng controlMO or 2ng MO2. Transverse, semi thin sections were stained with Toluidine Blue for histological analysis (A-D). From the same embryos, ultrathin sections were analyzed using transmission electron microscopy to visualize chondrocyte morphology and ECM structure. In I and K, the outline of a ceratobranchial arch 1 is indicated in blue. ch: ceratohyoid, cb 1- 5: ceratobranchial arches 1 - 5. Scale bars indicate 500 nm (E-L).

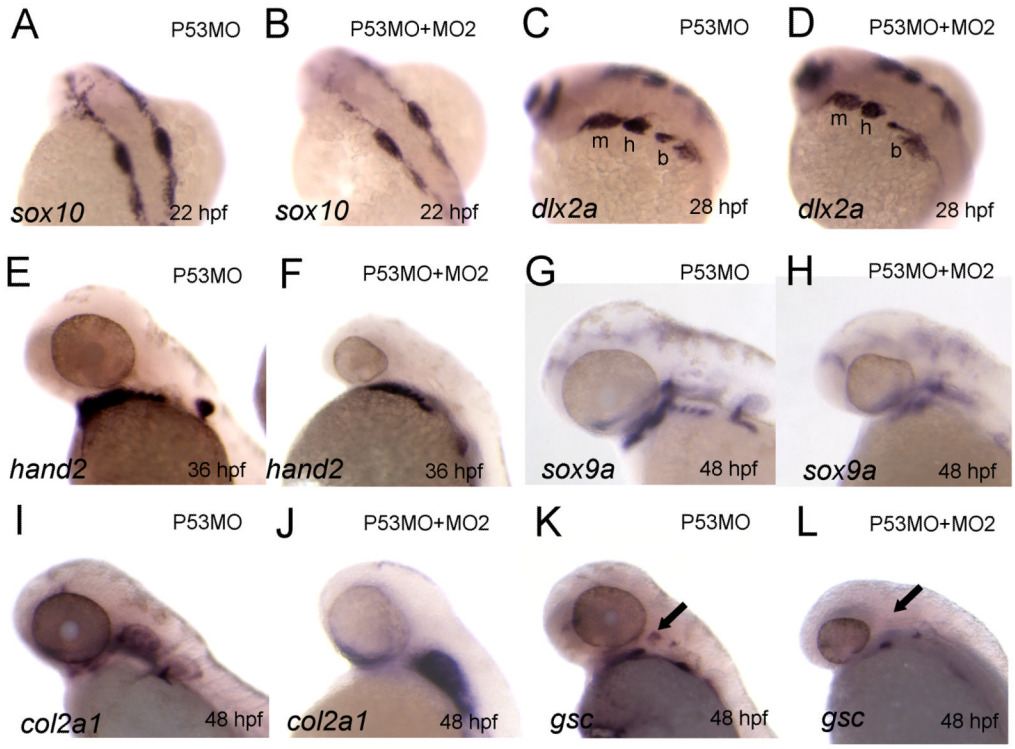

Fig. 6.

Chondrocyte condensation and differentiation but not early patterning is affected by *loxl3b* knockdown. A-L: *In situ* hybridization for various genes implicated in chondrogenesis at the indicated time points. Embryos were injected with either 2 ng P53MO (A, C, E, G, I, K) or 4 ng MO2 and 2 ng P53MO (B, D, F, H, J, L) morpholino. m: mandibular; h: hyoid; b: branchial; cb: ceratobranchial arches; black arrow: hyoid condensation.

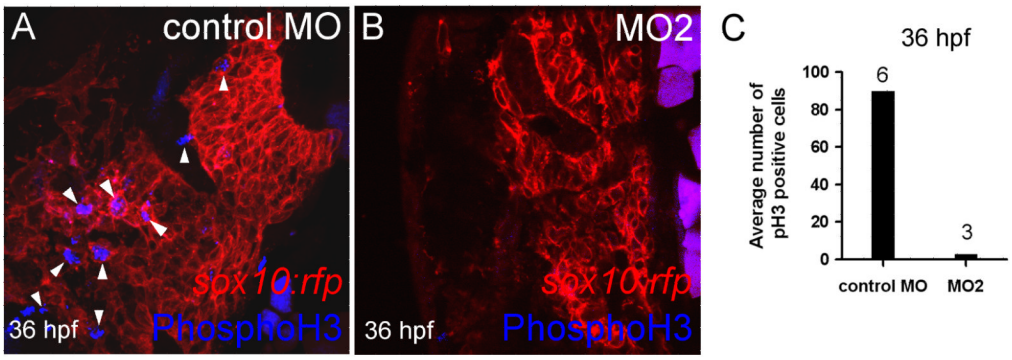

Fig. 7.

loxl3b is required for proliferation of chondrogenic progenitor cells. A, B: phosphohistone H3 expression is decreased in *sox10:rfp* transgenic embryos injected with control (A, arrowheads) versus MO2 (B) at 36 hpf. C: Quantification of phosphohistone H3 expression at 36 hpf in pharyngeal arch condensations of embryos injected with control or MO2. Depicted above the bars is the number of embryos examined.